

DOI: 10.1002/anie.200600400

**A Reaction–Diffusion Memory Device\*\***Akiko Kaminaga, Vladimir K. Vanag, and  
Irving R. Epstein\*

Any computer consists of processor and memory elements. Patterns and waves in excitable or oscillatory reaction–diffusion media are able to perform such processor tasks as counting,<sup>[1]</sup> logical operations,<sup>[2]</sup> signal transformation,<sup>[3]</sup> and finding the shortest path through a maze.<sup>[4]</sup> Since the brain may be thought of as a reaction–diffusion system, these capabilities are perhaps not so remarkable, though the simplicity of the systems employed is striking. Kuhnert et al.<sup>[5]</sup> demonstrated that the photosensitive Belousov–Zhabotinsky (BZ) oscillating chemical reaction is capable of briefly (for a few periods of oscillation, that is, several minutes) storing and smoothing an image as complex as a human face. However, practical applications require the ability to store information for longer periods of time, ideally indefinitely. Localized patterns in reaction–diffusion systems have been suggested as media for memory-storage devices.<sup>[6]</sup> The BZ system dispersed in a water-in-oil microemulsion (ME) with the surfactant sodium bis(2-ethylhexyl)sulfosuccinate (BZ-AOT system) exhibits a rich variety of pattern formation,<sup>[7]</sup> including several types of localized structures.<sup>[8]</sup> Herein we show that a photosensitive BZ-AOT system can store spatial information for up to an hour, even without replenishment of reactants. Simulation of this behavior with simple reaction–diffusion models reveals the likely mechanism of this information-storage capacity.

We recently reported the existence of localized stationary and oscillatory patterns in the BZ-AOT system.<sup>[8,9]</sup> In a system with tris(2,2'-bipyridine)ruthenium ( $[\text{Ru}(\text{bpy})_3]^{2+}$ ) catalyst, patterns can be suppressed by sufficiently intense illumination, which leads to photogeneration of bromide, an inhibitor of the reaction.<sup>[10]</sup> We have found conditions under which this system displays hysteresis and bistability (between a homogeneous steady state and stationary Turing patterns). Turing patterns, which are often invoked as a mechanism for biological morphogenesis, are spatially periodic concentration variations that arise as a result of the interaction between nonlinear reaction kinetics and diffusion.<sup>[11]</sup> Turing patterns form spontaneously in our system in the dark. If the light intensity ( $I$ ) is slowly increased, the patterns initially change

only slightly, but at a critical intensity ( $I_{\text{sc}}$ ), they suddenly vanish, and a homogeneous steady state (SS) is observed. If we then slowly decrease  $I$ , the Turing patterns spontaneously reemerge at a lower intensity ( $I_c$ ). For  $I_c < I < I_{\text{sc}}$ , the system is bistable, which is a characteristic feature of subcritical Turing instability. In this bistable range of  $I$ , localized patterns generated by a local perturbation can be stable, and Turing patterns cannot emerge spontaneously elsewhere in the medium, since the SS is also stable. First, we attempted to photoimprint an image and maintain it as long as possible for  $I$  within the bistable region, and then to develop a model that reproduces this phenomenon.

Since our BZ-AOT system is operated in a batch (closed system) mode, we first sought conditions under which stationary Turing patterns can survive for long periods of time (an hour or more) and the system displays significant photosensitivity. These criteria are fulfilled when  $[\text{MA}]_0 = 0.1 \text{ M}$ ,  $[\text{H}_2\text{SO}_4]_0 = 0.3 \text{ M}$ ,  $[\text{NaBrO}_3]_0 = 0.25 \text{ M}$ ,  $[\text{Ru}(\text{bpy})_3]_0 = 0.004 \text{ M}$ ,  $\omega = 10$ , and  $\varphi_d = 0.45$  (MA is malonic acid,  $\omega \equiv [\text{H}_2\text{O}]/[\text{AOT}]$  determines the radius of water droplets in the microemulsion, and  $\varphi_d$  is the volume fraction of the droplets). The radius of the water droplets, measured by dynamic light scattering, is 2 nm, and the microemulsion is below the percolation threshold, as shown by conductivity measurements in the range  $\varphi_d = 0.4\text{--}0.7$ . Under such conditions, the diffusion coefficient of small, oil-soluble molecules, such as the inhibitor  $\text{Br}_2$ , is significantly larger than that of water-soluble molecules, such as the activator  $\text{HBrO}_2$ , that diffuse with entire water droplets.<sup>[12]</sup>

When  $I$  is in the bistable region, the image of the mask imprinted in the layer of reactive ME can persist essentially unchanged for approximately 30 min. Since our system is closed, the concentrations of BZ reactants and intermediates evolve, and the photosensitivity, as characterized by, for example, the values of  $I_c$  and  $I_{\text{sc}}$ , also changes with time. To maintain the image of the mask for longer we must change the light intensity accordingly. This procedure extends the lifetime of the image to more than an hour, which is roughly the lifetime of the reactive ME in our batch configuration.

Figure 1 presents snapshots taken from a typical experiment. The image in Figure 1 A, which is taken shortly after decreasing  $I$  to within the bistable region, is essentially identical to the “face” mask through which the reactor is illuminated. The “face” image remains for about 1 h, but the continuous lines transform into dotted lines (Figure 1 A and B). Similar behavior is observed in the Turing patterns in the unilluminated area: most of the stripes that emerge initially mutate into spotlike Turing patterns after 30–60 min. If we increase  $I$  briefly (2–7 min) to suppress the image and then decrease it back to within the bistable region, the original image slowly reappears. Longer exposure to strong light erases the memory of the medium. If we decrease  $I$  below the bistable region, new spots begin to emerge around and within the “face” and eventually cover the entire area. Figure 1 C shows a space–time plot made from a cross section of Figure 1 B taken immediately after the light intensity was decreased. The emergence of new stationary spots is seen as the advent of vertical white bands.

[\*] Dr. A. Kaminaga, Dr. V. K. Vanag, Professor I. R. Epstein  
Department of Chemistry and  
Volen Center for Complex Systems, MS 015  
Brandeis University  
Waltham, MA 02454 (USA)  
Fax: (+1) 781-736-2516  
E-mail: epstein@brandeis.edu

[\*\*] This work was supported by grant CHE-0306262 from the Chemistry Division of the National Science Foundation and by the donors of the American Chemical Society Petroleum Research Fund.

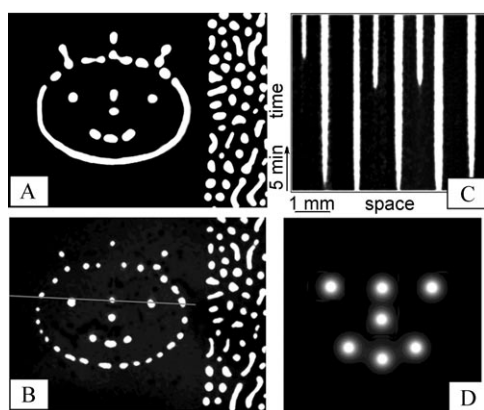


**Figure 1.** Images of the mask shown in Scheme 1 in the BZ-AOT system (A, B). Size of snapshots A and B is 7.7 mm × 5.8 mm. The time between frames A and B is 1 h.  $l = I_0/5$ ,  $I_0 = 28 \text{ mWcm}^{-2}$ . The right-hand side of the reactor (with Turing stationary spots) was not illuminated. C) Space–time plot for the experiment shown in A and B along the cross-sectional line marked in B taken immediately after the light intensity was decreased (bottom of frame C shows time = 0). New spots appear at roughly 10 (2 spots) and 14 min. D) Localized spots in the model described by Equations (1) and (2) with parameters  $f = 2$ ,  $q = 0.001$ ,  $m = 200$ ,  $\varepsilon_1 = 0.1$ ,  $i_0 = 0.025$ ,  $\varepsilon = 0.2$ ,  $D_v = 1$ ,  $D_z = 20$ , size = 100 × 100.

Various patterns in the BZ-AOT system, including Turing patterns, have been successfully simulated by several two-, three-, and four-variable models.<sup>[8,9,13]</sup> We have found localized patterns in all of these models with broad, but different, ranges of parameters.<sup>[14]</sup> Our simplest model is obtained by augmenting the two-variable Oregonator model<sup>[15]</sup> by a term  $i_0$  that accounts for the photoinduced production of bromide ion (inhibitor of autocatalysis)<sup>[16]</sup> and by introducing an additional term  $mz$  [Eqs. (1) and (2)].

$$\partial v / \partial \tau = ([fz + i_0(1 - mz)](q - v)) / (q + v) + v(1 - mz) / (1 - mz + \varepsilon_1 - v^2) / \varepsilon + D_v \nabla^2 v \quad (1)$$

$$\partial z / \partial \tau = v(1 - mz) / (1 - mz + \varepsilon_1) - z + D_z \nabla^2 z \quad (2)$$

In this model,  $v$  and  $z$  are dimensionless concentrations of activator (HBrO<sub>2</sub>) and oxidized catalyst, ( $[\text{Ru}(\text{bpy})_3]^{3+}$ ), respectively;  $D_v$  and  $D_z$  are dimensionless diffusion coefficients of activator and catalyst, respectively; and  $f$ ,  $\varepsilon$ , and  $q$  are parameters of the Oregonator model.<sup>[15]</sup> The term  $mz = [Z]/C_0$  ( $[Z]$  and  $C_0$  are the concentrations of oxidized and total (reduced plus oxidized) catalyst, respectively) takes into account that only the oxidized state of the catalyst is photosensitive and that autocatalysis ceases if  $mz$  approaches 1 ( $0 < \varepsilon_1 < 1$ ).<sup>[9]</sup>

We assume  $D_v \ll D_z$ , since the inhibitor bromine diffuses much more rapidly in the oil phase than the activator  $v$ , and its concentration is almost linearly related to that of the catalyst  $z$  through mass exchange and chemical transformations.<sup>[9,13,17]</sup> Figure 1 D shows a set of localized stationary spots (analogues

of the “eyes”, “nose”, and “mouth” of our imprinted image) modeled by Equations (1) and (2).

Computer simulations of Equations (1) and (2) reveal that the behavior of the localized spots as  $i_0$  is varied depends on  $D_z$  ( $D_v = 1$ ). The parametric diagram in Figure 2 A shows that

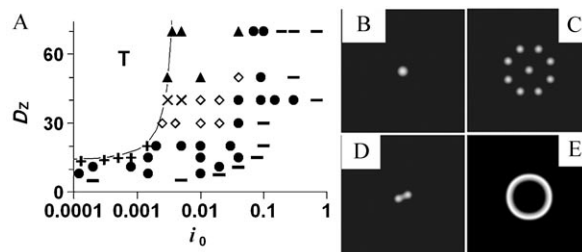


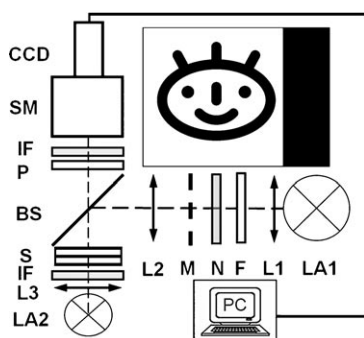
**Figure 2.** Parametric diagram in the  $i_0$ – $D_z$  plane (A) for Equations (1) and (2). Symbols: localized stationary spot ●; homogeneous SS ○. Turing instability occurs in domain T (calculated by linear stability analysis). The localized initial spot (B) can lose stability by producing new spots at radius  $R$  from the center (+) (C), by splitting into two spots (◇) (D), or by emitting a circular wave (▲) (E). The circular smooth wave loses its circular symmetry as it approaches the boundaries and transforms first into a dashed wave<sup>[20]</sup> and then emits backward waves. In a narrow parameter region (×), the circular wave is segmented into dashes. Parameters:  $f = 1.85$ ,  $q = 0.004$ ,  $m = 10$ ,  $\varepsilon_1 = 0.02$ ,  $\varepsilon = 0.4$ ,  $D_v = 1$ , size = 100 × 100.

at a small  $D_z$  value an initial localized spot (Figure 2 B) generates new spots lying on a circle when  $i_0$  is decreased (Figure 2 C); at a larger  $D_z$  value, the localized spot splits into two new spots (self-replication scenario)<sup>[18]</sup> (Figure 2 D); and at an even larger  $D_z$  value, the localized spot emits a circular wave (Figure 2 E). For all  $D_z$  values examined, the final stationary pattern for small values of  $i_0$  consists of spots occupying the entire area, whereas larger values of  $i_0$  lead to the homogeneous SS. Comparison with the experimental results (Figure 1 C), in which a decrease in  $i_0$  leads to the emergence of new spots without affecting the existing ones, demonstrates that the scenario that corresponds to our experiments is the generation of new spots at small  $D_z$  values.

We have shown that the BZ reaction can be used not only for image processing<sup>[5]</sup> but also for image storage, if the BZ-AOT system is employed to enable bistability between the homogeneous steady state and localized stationary (Turing) patterns. Our results imply that images can be stored indefinitely if the BZ reactants are continuously replenished, which can be accomplished with various types of unstirred flow reactors.<sup>[19]</sup> This photosensitive system can thus be used to create readable and rewriteable chemical memory. From a practical point of view, these findings should be of most importance in three-dimensional media, which have a large enough information capacity to accomplish significant tasks. Although it is uncertain whether a mechanism resembling that involved in the BZ-AOT system is employed for memory storage in living systems, the potential for artificial computational devices created using reaction–diffusion systems is clear.

## Experimental Section

The reactive ME was prepared in the usual way<sup>[7,8]</sup> by mixing two stock microemulsions (ME1 and ME2) containing MA with H<sub>2</sub>SO<sub>4</sub> and NaBrO<sub>3</sub> with [Ru(bpy)<sub>3</sub>]<sup>2+</sup>, respectively, and enough pure octane to give the desired value of  $\varphi_d$ . A small drop of the reactive ME was placed between two optical windows separated by an annular teflon gasket (Zefluor membrane) of thickness 80  $\mu$ m, inner diameter 25 mm, and outer diameter 47 mm. This arrangement constitutes our reactor (sandwich S in Scheme 1). Patterns were observed at room temperature (24 °C) through a microscope equipped with a digital CCD camera connected to a computer.



**Scheme 1.** Block scheme of the experimental setup. LA1 500 W actinic arc lamp; LA2 tungsten 100 W lamp; L1, L2, L3 lenses; F band-pass filter (400–500 nm) with maximum transparency at 450 nm; N neutral density filter; M mask (the “face” mask used in our experiments is shown in the top right corner); S sandwich with photosensitive BZ-AOT system; BS beam splitter; P polarizer; IF interference filter (450 nm); SM stereo microscope; CCD camera; PC computer. The mask was printed onto a transparency film with a laser printer.

The reactive ME in the reactor was kept in darkness for about 1 hour because of the long induction period for the autocatalytic oxidation of [Ru(bpy)<sub>3</sub>]<sup>2+</sup> by NaBrO<sub>3</sub>. After autocatalysis began, stationary Turing patterns emerged within 1–2 min in the right-hand portion of the reactor, which was kept in darkness throughout the experiment. At 10 min before the end of the induction period (which was measured in advance), the reactor was illuminated through a mask (M) (Scheme 1) at the maximum light intensity  $I_0$ , which suppresses the emergence of patterns in all illuminated areas. As soon as an image of the mask (like that shown in Figure 1 A) appeared, the mask was removed, and neutral density filters N were inserted to reduce  $I$ .

Received: January 30, 2006

Published online: March 29, 2006

**Keywords:** imprinting · localized patterns · memory · reaction–diffusion systems

- [1] J. Gorecki, K. Yoshikawa, Y. Igarashi, *J. Phys. Chem. A* **2003**, *107*, 1664–1669.
- [2] I. N. Motoike, A. Adamatzky, *Chaos Solitons Fractals* **2005**, *24*, 107–114.
- [3] N. G. Rambidi, K. E. Shamayaev, G. Y. Peshkov, *Phys. Lett. A* **2002**, *298*, 375–382.
- [4] O. Steinbock, A. Toth, K. Showalter, *Science* **1995**, *267*, 868–871.
- [5] L. Kuhnert, K. I. Agladze, V. I. Krinsky, *Nature* **1989**, *337*, 244–247.

- [6] a) S. Barland, J. R. Tredicce, M. Brambilla, L. A. Lugiato, S. Balle, M. Giudici, T. Maggipinto, L. Spinelli, G. Tissoni, T. Knodl, M. Miller, R. Jager, *Nature* **2002**, *419*, 699–702; b) P. Couillet, C. Riera, C. Tresser, *Chaos* **2004**, *14*, 193–198.
- [7] V. K. Vanag, I. R. Epstein, *Phys. Rev. Lett.* **2001**, *87*, 228301.
- [8] V. K. Vanag, I. R. Epstein, *Phys. Rev. Lett.* **2004**, *92*, 128301.
- [9] A. Kaminaga, V. K. Vanag, I. R. Epstein, *J. Chem. Phys.* **2005**, *122*, 174706.
- [10] H. J. Krug, L. Pohlmann, L. Kuhnert, *J. Phys. Chem.* **1990**, *94*, 4862–4866.
- [11] A. M. Turing, *Philos. Trans. R. Soc. London Ser. B* **1952**, *237*, 37–72.
- [12] L. J. Schwartz, C. L. DeCiantis, S. Chapman, B. K. Kelley, J. P. Hornak, *Langmuir* **1999**, *15*, 5461–5466.
- [13] V. K. Vanag, I. R. Epstein, *Phys. Rev. Lett.* **2002**, *88*, 088303.
- [14] Numerical simulations were carried out with the FlexPDE package (<http://www.pdesolutions.com>) with zero-flux boundary conditions. FlexPDE refines the triangular finite-element mesh until the estimated error in any variable is less than a specified tolerance, which we chose as  $5 \times 10^{-5}$ , at every cell of the mesh. Smaller tolerances did not change the results.
- [15] J. P. Keener, J. J. Tyson, *Phys. D* **1986**, *21*, 307–324.
- [16] S. Kadar, T. Amemiya, K. Showalter, *J. Phys. Chem. A* **1997**, *101*, 8200–8206.
- [17] Taking into account the reactions  $\text{Br}_2 + \text{malonic acid} \rightarrow \text{Br}^- + \text{bromomalonic acid}$  and  $\text{Br}_2 + \text{H}_2\text{O} \rightleftharpoons \text{HOBr} + \text{Br}^- + \text{H}^+$ , we can write  $\text{Br}_2 \rightleftharpoons \text{Br}^-$ , and in addition  $y \cong fz/(q+v)$ , in which  $y$  is the dimensionless concentration of bromide ion.
- [18] K. J. Lee, W. D. McCormick, J. E. Pearson, H. L. Swinney, *Nature* **1994**, *369*, 215–218.
- [19] a) Z. Noszticzius, W. Horsthemke, W. D. McCormick, H. L. Swinney, W. Y. Tam, *Nature* **1987**, *329*, 619–620; b) Q. Ouyang, J. Boissonade, J. C. Roux, P. De Kepper, *Phys. Lett. A* **1989**, *134*, 282–286; c) W. Y. Tam, W. Horsthemke, Z. Noszticzius, H. L. Swinney, *J. Chem. Phys.* **1988**, *88*, 3395–3396.
- [20] V. K. Vanag, I. R. Epstein, *Phys. Rev. Lett.* **2003**, *90*, 098301.